Polarization-Modulated Infrared Reflection Absorption Spectroscopic Studies of a Hydrogen-Bonding Network at the Air−Water Interface

Qun Huo,[†] Leila Dziri,[†] Bernard Desbat,[‡] K. C. Russell,[†] and Roger M. Leblanc*[,†]

Department of Chemistry, Center for Supramolecular Science, University of Miami, P.O. Box 249118, Coral Gables, Florida 33124, and Laboratoire de Physico-Chimie Moléculaire, University Bordeaux I, 33405 Talence, France

Received: November 11, 1998; In Final Form: February 2, 1999

The hydrogen-bonding network formed between a triaminotriazine amphiphile ($2C_{18}$TAZ, **1**) and complementary barbituric acid (BA, **2**) at the air−water interface is investigated by polarization-modulated infrared reflection absorption spectroscopy (PM-IRRAS). The molecular structure and orientation of the 1:1 hydrogen-bonding network at the air−water interface is revealed in this study. Without the addition of BA to the subphase, the NH_2 scissoring of $2C_{18}$TAZ appeared in the spectrum as a broad negative absorption band between 1660 and 1605 cm^{-1}, indicating its perpendicular orientation to the air−water interface. When BA was added to the subphase, the NH_2 scissoring absorption band from the triaminotriazine moiety disappeared due to the complementary hydrogen bonding of BA to the $2C_{18}$TAZ monolayer. The formation of the rigid 1:1 hydrogen-bonding network also resulted in the disappearance of one of the ring quadrant stretch absorption bands of the $2C_{18}$TAZ molecule. New bands which are attributed to the vibration of BA can be clearly seen. Particularly, the C═O stretch from BA shows up in the spectra as two negative absorption bands around 1700 cm^{-1}. The negative signature of these two bands suggests that the BA molecules are oriented in the hydrogen-bonding network with the C-2 carbonyl positioned vertically toward the air, and the C-4 and C-6 carbonyls directed into the water subphase. This is consistent with formation of an assembly which optimizes the use of complementary hydrogen bonding between two components. Furthermore, the effect of competitive polar organic solvents in subphase, such as DMSO, on the hydrogen-bonding network has also been observed in this study. Compared to the previous IRRAS studies on the similar monolayers, the sensitivity of PM-IRRAS is obviously improved. PM-IRRAS will likely become a powerful analytical technique for the characterization of molecular structure and orientation of Langmuir monolayers at the air−water interface.

Introduction

Hydrogen bonding has crucial importance in many chemistry research areas. Despite its long history of being well studied by physical chemists and biochemists, it keeps attracting keen interest from synthetic chemists. Numerous artificial molecular recognition systems can be designed by incorporating complementary hydrogen bond donors and acceptors into host and guest molecules.[1−8] These artificial systems function as convenient and direct models to mimic complicated biological activities. Recently, these studies have been further expanded to the air−water interface.[9] Considering the significance of cell and biomembranes in biological systems, Langmuir monolayer techniques have become important model systems to mimic biological functions taking place at the membrane interfaces.

Among the different intermolecular interactions (e.g., electrostatic, hydrogen bonding, van der Waals, and $\pi-\pi$ stacking), the strength, directionality, and selectivity of hydrogen bonding places it at the center of many research efforts aimed at the design of supermolecules and crystal engineering through noncovalent synthesis. One notable example among these studies is the formation of supermolecules through complementary hydrogen-bonding self-assembly. It was found that barbiturates or cyanurates could self-assemble into highly organized structures such as linear tapes, crinkle tapes, or rosettes with complementary hydrogen-bonding melamines in the solid state or solution.[10−18] More recently, the formation of hydrogen-bonding networks between these complementary components has also been investigated in 2-D at the air−water interface.[19,20] Traditionally, it was believed that hydrogen bonding directed molecular recognition is difficult in polar media, such as water, due to the competition from the latter. However, in these recent studies, it has been shown that hydrogen-bond-directed self-assembly at the air−water interface is as efficient as that in nonpolar organic solvents. These investigations will likely become an important new approach in the design of novel artificial biomembranes and supermolecules in 2-D.

We have recently reported the study of a complementary hydrogen-bonding network formed between a 2-amino-4,6-dioctadecylamino-1,3,5-triazine ($2C_{18}$TAZ, **1**) monolayer with barbituric acid (BA, **2**) from the aqueous subphase at the air−water interface (Figure 1).[21] Brewster angle microscopy and in situ UV−vis absorption spectroscopy, respectively, have been used to observe the topography and the absorption spectra changes of the $2C_{18}$TAZ monolayer brought by the binding of BA. However, the molecular structure and orientation of this hydrogen-bonding network remains unclear from these studies. To have a full understanding of the structure of this hydrogen-

* To whom correspondence may be addressed. Tel: (305) 284-2282. Fax: (305) 284-4571. Email: rml@umiami.ir.miami.edu.
[†] Department of Chemistry.
[‡] Laboratoire de Physico-Chimie Moléculaire.

10.1021/jp984389c CCC: $18.00
Published on Web 03/30/1999

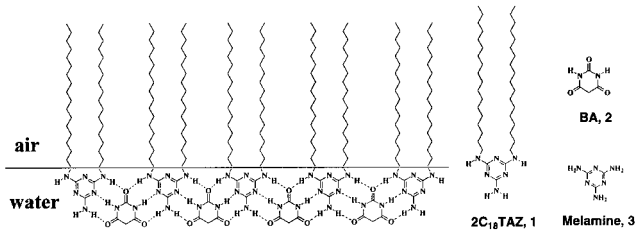

Figure 1. The 1:1 complementary hydrogen-bonding network formed between a $2C_{18}$TAZ monolayer and BA from aqueous subphase at the air−water interface.

bonding network, a more precise and detailed characterization at the molecular level is badly needed.

Infrared reflection absorption spectroscopy (IRRAS) has been used previously to characterize the hydrogen-bonding network between a C_{12} alkyl chain disubstituted triaminotriazine amphiphile ($2C_{12}$TAZ) and barbituric acid (BA) on Langmuir−Blodgett films.[19c] A new absorption peak which can be readily assigned to the C═O stretch from BA molecules appeared at 1719 cm^{-1} in the $2C_{12}$TAZ LB film when deposited from 10 mM BA subphase compared to the LB film deposited from the pure water subphase. However, it was noticed that the intensity of the absorption bands from the triaminotriazine (TAZ) headgroups is significantly decreased. More information regarding the conformational change of TAZ moiety from these spectra is not available. The orientation of the two complementary hydrogen-bonding components within the network remains unclear. More importantly, the information of molecular orientation and structure of monolayers obtained from their Langmuir−Blodgett films is not equivalent to the studies conducted directly at the air−water interface.

IRRAS has been a leading spectroscopic method for the in situ characterization of Langmuir monolayers at the molecular level.[22] Weck et al.[20c] has used this technique at the air−water interface to study the hydrogen bonding between a barbituric acid lipid monolayer and triaminopyrimidine (TAP) from the aqueous subphase. However, in general, the quality of these spectra is not ideal, even after significantly long acquisition times (5000 scans per spectrum). Further interpretation and analysis are difficult to conduct based on these spectra.

The main problem of IR spectroscopy at the air−water interface is extracting the very weak monolayer signal from the very strong absorptions occurring in the liquid subphase and especially, in the surrounding water vapor. Conventional IRRAS requires long acquisition times (more than 2000 scans) and continuous strict control of the vapor pressure during sample and reference (uncovered water) spectrum recording. Furthermore, the determination of molecular orientation at the air−water interface through traditional IRRAS has been shown to be considerably difficult and complicated.[23] The spectral intensities of the studied monolayer films have to be determined either with p-polarization at several angles of incidence or with both s- and p-polarized radiation at a single angle of incidence. Subsequently, a theoretical optical model is applied to calculate the orientation of the functional groups giving rise to the IR bands. The parameters of the optical model and the experimental setup must have been precisely pretested and characterized by using a known and well-defined monolayer system. In particular, the overall degree of polarization for the experimental setup must be accurately known due to its significant impact on the intensity of bands during studies with p-polarized irradiation.

To overcome these problems and difficulties, a differential IR reflectivity technique, polarization modulated infrared reflection absorption spectroscopy, PM-IRRAS, based on a rapid modulation of the polarization of the incident electromagnetic field on the sample has been developed.[24,25] Basically, PM-IRRAS combines Fourier transform mid-IR reflection spectroscopy with fast polarization modulation of the incident beam (ideally between p- and s-linear states). A two-channel electronic and mathematical processing of the detected signal is used in order to get the differential reflectivity spectrum:

$$\frac{\Delta R}{R} = \frac{R_p - R_s}{R_p + R_s}$$

R_p and R_s are the polarized reflectivities of the sample. Owing to the fast polarization modulation and to the identical and precise real time acquisition and processing of the two interferograms, this ratio is, in principle, extracted from all the polarization-independent signals (such as strong water vapor absorptions) and from all the instrumental drifts and fluctuations. In other words, the spectra obtained in this mode have a total immunity against the isotropic IR absorptions of the sample environment. The sensitivity of the technique is therefore greatly enhanced. More importantly, due to its differential nature, PM-IRRAS can distinguish between in-plane and out-of-plane vibrations. Vibrations which induce the transition moment changes along the horizontal direction (parallel to the water surface, in-plane) induce positive bands in the absorption spectra, while vibration modes causing the transition moment changes perpendicular to the aqueous subphase (out-of-plane) result in negative absorption bands. When the incidence angle of the PM-IRRAS signal is set at an optimized value (75° for pure liquid water subphase), the highest signal/noise ratio is obtained for the detection of absorptions both with in-plane and out-of-plane transition moments.

Recently, this newly developed technique has been successfully applied to the study of arachidic acid, arachidate, dimyristolyl phosphatidylcholine (DMPC), polypeptidic melittin and other monolayers at the air−water interface.[25] The average acquisition time for these spectra is around 200−300 scans (ca. 10 min), greatly faster than the traditional IRRAS. In addition, the quality of the spectra are significantly improved. Further conformational and structural analysis can be readily conducted based on these spectra. For example, it was shown that, in the spectra of an arachidate monolayer,[24,25] the asymmetric $\nu_a COO^-$, which causes the horizontal transition moment, gives a positive absorption band at 1540 cm^{-1} and the symmetric $\nu_s COO^{-1}$, which causes the vertical transition moment, gives a negative absorption band at 1445 cm^{-1}. Thus, information of how the arachidate headgroup is anchored was obtained.

In this report, we present our exploration of using this sensitive technique to study the hydrogen-bonding network formed between a $2C_{18}$TAZ monolayer and BA at the air−water interface. The molecular structure and orientation of the hydrogen-bonding network formed at the air−water interface has been readily revealed through the analysis of its PM-IRRAS spectra.

Experimental Section

The PM-IRRAS studies of $2C_{18}$TAZ monolayer at the air−water interface has been conducted following a very similar instrumental setup and experimental procedure as described previously.[25] PM-IRRAS spectra have been recorded on a Nicolet 740 FT-IR spectrometer. The 1 mM solution of $2C_{18}$-TAZ in $CHCl_3$ (Aldrich, HPLC grade) was spread on a simple homemade 25 cm × 5 cm LB trough, milled in Kel-F and equipped with an adjustable moving barrier. The subphase is

TABLE 1: Characteristic Absorption Frequencies for Melamine and $2C_{18}$TAZ in Different Environments

	state	NH_2 scissors (cm^{-1})	ring quadrant stretch (cm^{-1})	ring semicircle stretch (cm^{-1})
melamine[a]	calculated frequency by *ab initio* method	1593 s[b]	1593 s, 1563 m	1432 m
	gas phase	1598 s	1598 s, 1566 m	1440 m
	solid state	1563 vs 1627 sh	1580 sh 1550 vs	1467 m 1436 s
$2C_{18}$TAZ	$CHCl_3$ solution	1577 s	1577 s 1515 s	1480 sh 1463 m 1430 sh 1353 w
	thin solid film	1678 w 1607 m	1581 s 1527 vs	1480 sh 1468 m 1428 sh 1366 m
	KBr pellet	1641 m	1593 vs	1456 w 1415 m 1358 m
	air−water interface	1607 m	1580 s 1531 vs	1470 m 1434 w 1366 m

[a] The absorption frequencies for melamine are cited from reference 26. [b] vs: very strong; s: strong; sh: shoulder; m: medium; w: weak.

milliQ-filtered (MILLIPORE) ultrapure water. Three subphases have been used in the study, pure water, 1 mM BA in water and 1 mM BA in water/DMSO (v/v 80/20). The purpose of adding DMSO to the subphase is to verify if the strong solvating ability of DMSO can disrupt the formation of the hydrogen-bonding network, as shown by Brewster angle microscopy studies.[21] The PM-IRRAS absorption spectra of $2C_{18}$TAZ monolayer on the three subphases have been taken at a surface pressure of 25 mN/m with a 4 cm^{-1} resolution by coadding 400 scans (ca. 15 min) and are presented as a normalized difference vs the spectrum of the uncovered subphase obtained under the same conditions.

Since not reported previously, the IR spectra of $2C_{18}$TAZ in $CHCl_3$ solution, thin solid film, KBr pellet, and its Raman spectrum have also been recorded. The thin solid film of $2C_{18}$-TAZ was formed by simply applying one drop (ca. 0.01 mL) of 1 mM $2C_{18}$TAZ solution on the surface of the CaF_2 cell and waiting 10 min to allow evaporation of the solvent. The IR spectra of $2C_{18}$TAZ in $CHCl_3$ solution and as a thin solid film have been obtained from a Perkin-Elmer PE-GRAMS/2000 FT-IR spectrometer with a resolution of 2 cm^{-1} and coadding 200 scans per spectrum. The IR spectrum of $2C_{18}$TAZ in KBr pellet (2 mg $2C_{18}$TAZ in 300 mg KBr were milled together) has been recorded with a Nicolet 740 spectrometer with 4 cm^{-1} spectral resolution and by coadding 200 scans. The Raman spectrometer is a "Labram" Dilor spectrometer with a He−Ne laser. The spectrum was obtained with a 2 min integration time at a 4 cm^{-1} spectral resolution.

Results and Discussion

The assignment of the absorption bands of $2C_{18}$TAZ molecules (Table 1) has been accomplished by the comparison with the IR spectra of melamine (**3**, for structure, see Figure 1).[26,27,28] Since the $2C_{18}$TAZ is a dialkylsubstituted melamine, we assume the IR spectrum of $2C_{18}$TAZ should have some common features with melamine. Although melamine is a well-known compound, the assignment of its IR absorption bands was only recently completed with the aid of theoretical vibrational calculations.[26] Two intense infrared peaks are observed for melamine at 1593−1598 cm^{-1} and 1438−1440 cm^{-1} in both the gas phase and solid argon matrix. By comparing the theoretical calculation and analysis of deuterated melamine spectra, the first band is assigned to the scissoring of the three NH_2 groups and the stretching of the triazine ring, while the second band is assigned to the ring and side chain CN stretching. Between the two most intense bands, there is a strong feature at 1556 cm^{-1} (gas phase) or 1561 cm^{-1} (matrix) due to NCN bending coupled with ring deformation. In the gas phase and solid argon matrix, the NH_2 scissoring absorption band overlaps with one of the ring stretching absorption bands (1598 cm^{-1}). One notable feature of the melamine spectra is that the NH_2 scissoring is strongly dependent on hydrogen bonding. The hydrogen-bond donor group (NH_2) of melamine is able to form hydrogen bonds with the hydrogen-bonding acceptor group (nitrogen in the *s*-triazine ring) from another melamine molecule in the solid state. When such a hydrogen bond is formed, the NH_2 scissoring vibration occurs with higher vibrational energy, and the absorption band shifts to higher frequency. Indeed, it was found that, in solid state, the NH_2 scissoring appears at 1653 cm^{-1}. Comparing this to the gas phase and solid argon matrix, the absorption band is shifted to a higher frequency by about 60 cm^{-1}, well separated from the ring stretch absorption band at 1598 cm^{-1}.[26,27]

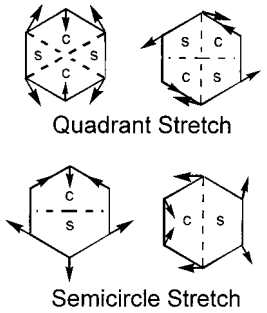

Figure 2. An illustration of the quadrant and semicircle ring stretch of aromatic and heteroaromatic rings. C: contract; S: stretch.

It has been described that the ring stretches for aromatic and heteroaromatic rings can be divided into two different modes, the quadrant stretch and the semicircle stretch, as illustrated in Figure 2.[29a,b] In the quadrant stretch, two-quarters of the ring contract while the other two-quarters of the ring stretch. In the semicircle stretch mode, half part of the ring contracts while the other part of the ring stretches, causing the ring stretch and deformation. The quadrant stretch of *s*-triazine ring lead to an absorption band around 1555 cm^{-1} while the semicircle stretch results in an absorption frequency around 1410 cm^{-1}.[29b] Each of these two bands may be doubled if the *s*-triazine ring is substituted, giving rise to multiple ring stretch bands around this region.

As mentioned earlier, the $2C_{18}$TAZ molecule is a dialkyl-substituted melamine. The NH_2 scissoring and ring stretch absorption bands of $2C_{18}$TAZ need to be identified first. In dilute $CHCl_3$ solution (Figure 3a), there are two strong bands around the region of 1600−1500 cm^{-1} and multiple bands at 1450−1350 cm^{-1}. The band at 1577 cm^{-1} can be assigned as the NH_2 scissoring and one of the *s*-triazine quadrant ring stretches of the $2C_{18}$TAZ, while the band at 1515 cm^{-1} can be assigned as another quadrant ring stretch. The multiple bands appearing at

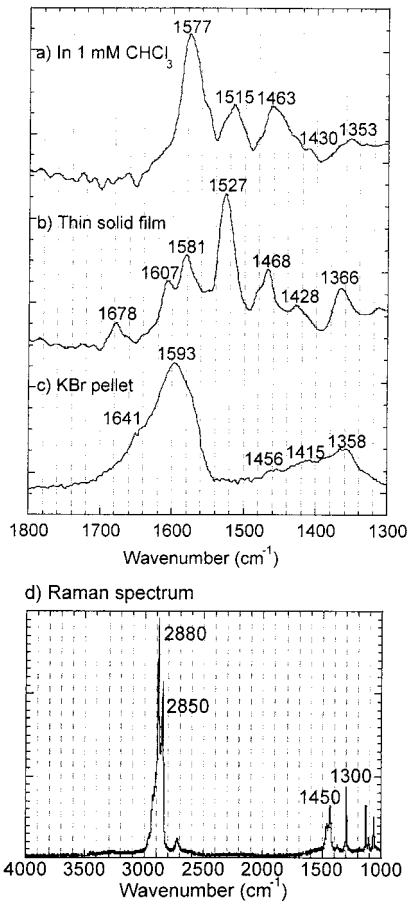

Figure 3. The FT-IR spectra of $2C_{18}TAZ$ in $CHCl_3$ solution (a), thin solid film (b), KBr pellet (c), and its Raman spectrum in pure powder (d).

1450−1350 cm^{-1} can be attributed to the semicircle ring stretch and the side chain CN stretch of the $2C_{18}TAZ$ molecule. In the thin solid film (Figure 3b), the multiple bands at 1450−1350 cm^{-1} did not show a significant shift when compared to those in dilute $CHCl_3$ solution. However, the absorption bands around 1600−1500 cm^{-1} shifted significantly and two new bands appeared at higher frequency (1678 and 1607 cm^{-1}). Comparison with the NH_2 scissoring of melamine in solid state indicates these two new bands can be assigned to the NH_2 scissoring of $2C_{18}TAZ$. The absence of these bands in dilute solution and the presence of these bands in solid state indicate that the NH_2 group from one $2C_{18}TAZ$ molecules is hydrogen bonded with another $2C_{18}TAZ$ molecule, just as described for melamine. Since the nitrogen atoms from the aromatic ring have to participate to form this hydrogen-bonding network, some of the ring stretch vibrations are also affected by this hydrogen bonding. One ring quadrant stretch band shifted from 1515 to 1527 cm^{-1} and another ring quadrant stretch band shifted from 1577 to 1581 cm^{-1}. The semicircle ring stretching bands around 1450−1350 cm^{-1} remain at almost the same frequencies. In the KBr pellet (Figure 3c), the same trend was observed. The band around 1600 cm^{-1} is very broad, and two peaks are discernible, 1593 and 1641 cm^{-1}. The 1641 cm^{-1} band can be attributed to the NH_2 scissoring and the 1593 cm^{-1} band is due to the quadrant ring stretch. The multiple bands at 1450−1350 cm^{-1} region are due to the semicircle ring stretch and remain at almost the same frequencies as in dilute $CHCl_3$ solution and in thin solid films.

The Raman spectrum of $2C_{18}TAZ$ pure powder (Figure 3d) has confirmed the structure of the $2C_{18}TAZ$ molecule. Two

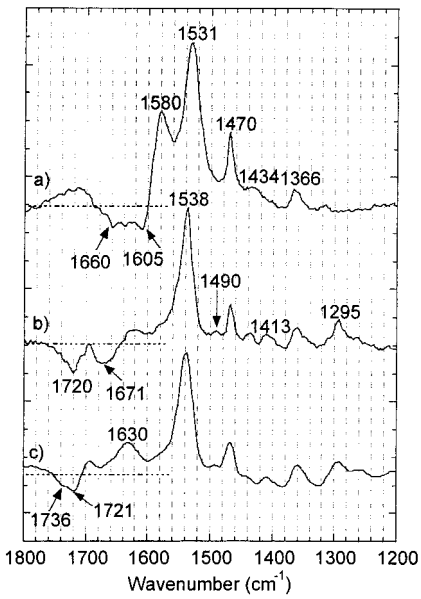

Figure 4. The PM-IRRAS spectra of $2C_{18}TAZ$ at the air−water interface on different subphases: (a) pure water, (b) 1 mM BA in pure water, (c) 1 mM BA in water/DMSO (v/v 80/20). The *y*-axis is the PM-IRRAS signal with arbitrary unit. The dotted line indicates the approximate zero level of PM-IRRAS signal (i.e., $R_p = R_s$).

strong absorption bands can be seen at 2880 and 2850 cm^{-1} which are due to CH stretch. The NH_2 scissoring gave no detectable Raman band, which is typical of aromatic amine compounds.[29c] The medium absorption band appearing at 1450 cm^{-1} is assigned to the quadrant stretch of the *s*-triazine ring and the absorption band at 1300 cm^{-1} can be assigned to the semicircle stretch of the *s*-triazine ring. Since the NH_2 scissoring absorption is not detectable, the Raman spectrum is unfavorable to look at the changes in the hydrogen-bonding network.

Figure 4 is the PM-IRRAS spectra of $2C_{18}TAZ$ monolayer at the air−water interface on different subphases. Compared to the spectra obtained by conventional IRRAS at the air−water interface on related studies,[20c] the quality of the spectra is improved, while at the same time the acquisition time is largely reduced. The spectrum of $2C_{18}TAZ$ on the pure water subphase (Figure 4a) is quite similar to the one obtained from its thin solid film. Considering that the spectrum of the monolayer was taken in a solid-condensed phase (25 mN/m), this result seems very reasonable. The multiple semicircle stretch bands, 1470, 1434, and 1366 cm^{-1}, appeared almost at the same position as in dilute $CHCl_3$ solution, thin solid film, and KBr pellet. The two quadrant ring stretches (1580 and 1531 cm^{-1}) also appeared at the same position as in the thin solid film (1581 and 1527 cm^{-1}). The NH_2 scissoring can be found between 1660 and 1605 cm^{-1} as a broad negative band, also corresponding to the NH_2 scissoring in the thin solid film.

As described earlier, PM-IRRAS can distinguish the horizontal transition moment from the perpendicular transition moment. If a TAZ polar headgroup with a C_{2v} symmetry axis is oriented perpendicular to the water surface, one can see that the NH_2 scissoring will only cause the transition moment change in the direction perpendicular to the water surface (Figure 5), which results in a negative absorption band. In other words, the observation of the NH_2 scissoring as a negative band further confirms the perpendicular orientation of the $2C_{18}TAZ$ molecules to the water surface.

The appearance of the NH_2 scissoring band at the same position at the air−water interface as in thin solid film suggests that the NH_2 group from one $2C_{18}TAZ$ molecule formed

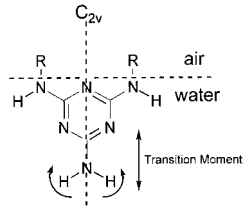

Figure 5. An illustration of the perpendicular orientation of $2C_{18}$TAZ to the water surface and the NH_2 scissoring vibration mode.

hydrogen bonding with another $2C_{18}$TAZ molecule or with water in the monolayer. Our previous studies by UV−vis absorption spectroscopy[21] has shown that the $2C_{18}$TAZ molecules formed an irreversible monolayer at the air−water interface. The irreversibility of the monolayer was attributed to strong intermolecular interactions between the TAZ polar headgroups or between the TAZ moieties with water molecules. Combining these experimental results, we have concluded that a stable hydrogen-bonding network is most likely formed between the $2C_{18}$TAZ molecules with the participation of water molecules. Due to this hydrogen bonding effect, the NH_2 scissoring absorption band shifted to higher frequency. The appearance of a dispersive shape of the base line between 1720 and 1660 cm^{-1} is more probably due to the H−O−H bending of organized and oriented water molecules at the interface, as discussed in the previous works.[24,25]

The spectrum of the $2C_{18}$TAZ monolayer on the 1 mM BA subphase (Figure 4b) shows obvious differences from the pure water subphase. First, two bands from the $2C_{18}$TAZ molecule have totally disappeared (the broad negative band between 1660 and 1605 cm^{-1} and the positive band at 1580 cm^{-1}), and several new bands appeared. The new bands can be easily assigned to the BA molecules. The new peaks between 1250 and 1500 cm^{-1} (1490, 1413, and 1295 cm^{-1}) are attributed to the C−N stretch and C−H bending of the BA molecules. The two negative bands appearing at 1671 and 1720 cm^{-1} can be attributed to the C═O stretch of the BA molecules. The appearance of these new bands is strong evidence for the binding of BA molecules from subphase to the $2C_{18}$TAZ monolayer.

The absorption frequency of the C═O stretch from BA is strongly dependent on hydrogen bonding. The C═O peak of BA in an argon matrix appears at 1754 cm^{-1} for the monomer and 1732 cm^{-1} for the dimer. These peaks shift to 1694 cm^{-1} in the solid state at 20 K, owing to hydrogen-bond formation between BA molecules.[30] It was also reported that in aqueous solution, the C═O stretches of BA appear at 1750, 1720 and 1704 cm^{-1}. When mixed with a complementary component, such as triaminopyrimidine (TAP), in a 1:1 ratio in water, the carbonyl stretch shifted to lower frequency at 1673 cm^{-1}.[20a] A shift in the C═O peak of a BA derivative has also been reported in KBr pellet, from 1737 to 1715 cm^{-1}.[31] The formation of the hydrogen bonds weakens C═O bond strength, and the C═O stretch occurs at lower vibrational energy. For the $2C_{18}$TAZ monolayer on BA subphase, the appearance of the C═O stretch absorption band of BA molecules at 1720 and 1671 cm^{-1} in the PM-IRRAS spectra verified the existence of hydrogen bonding between BA and TAZ moieties at the air−water interface.

Another noteworthy point needed be discussed is the negative signature of these two bands. To bind with $2C_{18}$TAZ molecules complementarily with six-point hydrogen bonding, the BA molecules will have to orient themselves in the direction as shown in Figure 6, with the C-2 carbonyl group oriented vertically toward the air, and the C-4 and C-6 carbonyl groups oriented toward the water subphase. The three carbonyl groups

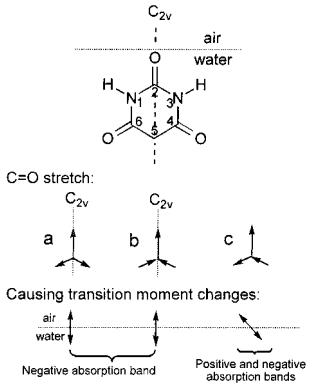

Figure 6. An illustration of the orientation of BA molecule in the hydrogen-bonding network and the transition moment changes caused by the symmetrical or antisymmetrical stretch of three C═O groups.

in BA can vibrate symmetrically (Figure 6a and b) or antisymmetrically (Figure 6c) to give multiple or broad absorption bands.[29d] With the orientation of BA molecules shown in Figure 6, the C_{2v} symmetry axis of BA molecule is normal to the water surface and the two C_{2v} symmetrical stretches of the three C═O bonds can only cause transition moment changes perpendicular to the water surface, which leads to two negative absorption bands. On the other hand, the antisymmetrical stretch of the three C═O groups shown in Figure 6c may cause transition moment changes both along the horizontal and perpendicular direction, which leads to both positive and negative absorption bands. However, there is no discernible positive band appeared in this region from 1750 to 1600 cm^{-1}. One possibility is that the positive band might be overlapping with other absorption bands. The other possibility is this vibration mode becomes inactive in the hydrogen-bonding network compared to its nonbonded state. The antisymmetrical vibration of the three C═O groups shown in Figure 6c will disrupt the C_{2v} symmetrical linear hydrogen-bonding network, which is energetically unfavorable. The absorption intensity of this vibration mode is therefore decreased to a nondetectable level.

The analysis of the absorption bands arising from the TAZ polar headgroups is also very informative. Two bands from $2C_{18}$-TAZ molecules disappear, the negative NH_2 scissoring band around 1660 to 1605 cm^{-1} and one of the positive ring stretch bands at 1580 cm^{-1}. The disappearance of these two bands is attributed to the presence of a rigid hydrogen-bonding network. As shown in Figure 1, once the TAZ moiety forms a complementary hydrogen-bonding network with BA by six-point hydrogen bonding, the NH_2 scissoring vibration becomes inactive. It was noticed previously for melamine compounds that, if all NH_2 groups are replaced by NHR or NR_2 groups, the NH_2 scissoring absorption band disappears.[29b] The formation of hydrogen bonds between NH_2 groups with C═O from BA can be envisaged as a disubstitution of the two protons on the NH_2 groups. Similar phenomena have also been found in the 1:1 complementary hydrogen-bonding assembly of BA and TAP in aqueous solution.[20a] For pure TAP in water, the NH_2 scissoring absorption band appears at 1620 cm^{-1}. When mixed with BA in a 1:1 ratio in water, this band completely disappeared. The disappearance of absorption band at 1580 cm^{-1} of the $2C_{18}$TAZ monolayer on the BA subphase is due to the same reason. As explained earlier, the nitrogen atoms in the *s*-triazine ring have to participate in the hydrogen-bonding network as hydrogen bond acceptors. This will cause some of the ring stretching vibrations to become inactive. The absorption bands resulted from these vibration modes disappear.

Furthermore, the effects of the addition of a polar organic solvent, DMSO, to the subphase on the hydrogen-bonding network was also investigated by this technique. As concluded from our previous work, the addition of a polar solvent such as DMSO to the subphase partially disrupts the formation of hydrogen-bonding network between $2C_{18}$TAZ monolayer and BA. This is due to the strong solvation of the TAZ polar headgroups and BA by DMSO. Figure 4c shows the PM-IRRAS spectra of $2C_{18}$TAZ monolayer taken from 1 mM BA in water/DMSO (v/v 80/20) subphase. Some discernible changes have been brought by the addition of DMSO. First, the relative intensity of the absorption bands of BA molecules to the $2C_{18}$-TAZ monolayer absorption bands is decreased in the water/DMSO subphase, indicating fewer BA molecules binding to the monolayer. Second, there are some obvious shifts of the C═O stretch absorption bands. The two negative bands appeared at higher frequencies, 1736 and 1721 cm^{-1} on water/DMSO subphase, compared to the 1720 and 1671 cm^{-1} on the pure water subphase. The shift of the C═O stretch of BA to higher frequencies indicates a weaker hydrogen bonding effect. More importantly, there is a new positive band appearing at 1630 cm^{-1}. Due to the partial disruption of the hydrogen-bonding network, the BA molecules regain more freedom in a less rigid structure. Some of the vibration modes which are inactive in the network, such as the antisymmetrical stretch of three C═O groups from BA, may become active again, giving rise to absorption bands such as the one at 1630 cm^{-1}, with detectable intensities. All in all, the appearance and disappearance of absorption bands from the C═O stretch strongly suggests a different organization and orientation of BA molecules on water subphase from water/DMSO mixed subphase.

In summary, the present study describes a newly developed analytical technique, PM-IRRAS, for the study and characterization of molecular structure and orientation of monolayers at the air−water interface. Compared to the conventional IRRAS, the sensitivity of the technique is greatly increased. Within much shorter acquisition time (less than 500 scans for PM-IRRAS vs more than 2000 scans for conventional IRRAS), high quality spectra can be obtained and further analysis is readily conducted based on these spectra. For the first time, the structure and molecular orientation of a hydrogen-bonding network formed between a $2C_{18}$TAZ monolayer and BA from aqueous subphase at the air−water interface has been much more clearly characterized and verified from their PM-IRRAS spectra. These studies will help in the future design of supermolecules using hydrogen bond as noncovalent synthetic tool. It is expected that this highly sensitive and informative molecular characterization technique will become an extremely important and powerful analytical tool in surface chemistry research, especially in the study of molecular recognition at the air−water interface to mimic the biological function of cell and biomembranes.

Acknowledgment. This work is based upon work supported by the US Army Research Office under Contract 36479_CH.

References and Notes

(1) Tecilla, P.; Chang, S. K.; Hamilton, A. D. *J. Am. Chem. Soc.* **1990**, *112*, 9586−9590.

(2) Slobodkin, G.; Fan, E.; Hamilton, A. D. *New. J. Chem. Res.* **1992**, *16*, 643−645.

(3) Ghadiri, M. R.; Granja, J. R.; Milligan, R. A.; McRee, D. E.; Khazanovich, N. *Nature* **1993**, *366*, 324−327.

(4) Fan, E.; Van Arman, S. A.; Kincaid, S.; Hamilton, A. D. *J. Am. Chem. Soc.* **1993**, *115*, 369−370.

(5) Rotello, V. M.; Viani, E. A.; Deslongchamps, G.; Murray, B. A.; Rebek, J., Jr. *J. Am. Chem. Soc.* **1993**, *115*, 797−798.

(6) Kinbara, K.; Hashimoto, Y.; Sukegawa, M.; Nohira, H.; Saigo, K. *J. Am. Chem. Soc.* **1996**, *118*, 3441−3449.

(7) Munakata, M.; Wu, L. P.; Yamamoto, M.; Kuroda-Sowa, T.; Maekawa, M. *J. Am. Chem. Soc.* **1996**, *118*, 3117−3124.

(8) Branda, N.; Kurtz, G.; Lehn, J.-M. *Chem. Commun.* **1996**, 2443−2444.

(9) Paleous, C. M.; Tsiourvas, D. *Adv. Mater.* **1997**, *9*, 695−710.

(10) Zerkowski, J. A.; Seto, C. T.; Weirda, D. A.; Whitesides, G. M. *J. Am. Chem. Soc.* **1990**, *112*, 9025−9026.

(11) Zerkowski, J. A.; Seto, C. T.; Whitesides, G. M. *J. Am. Chem. Soc.* **1992**, *114*, 5473−5475.

(12) Seto, C. T.; Whitesides, G. M. *J. Am. Chem. Soc.* **1993**, *115*, 905−916.

(13) Zerkowski, J. A.; Whitesides, G. M. *J. Am. Chem. Soc.* **1994**, *116*, 4298−4304.

(14) Zerkowski, J. A.; Mcdonald, J. C.; Seto, C. T.; Wierda, D.; Whitesides, G. M. *J. Am. Chem. Soc.* **1994**, *116*, 2382−2391.

(15) Zerkowski, J. A.; Mathias, J. P.; Whitesides, G. M. *J. Am. Chem. Soc.* **1994**, *116*, 5305−5315.

(16) Zerkowski, J. A.; McDonald, J. C.; Whitesides, G. M. *Chem. Mater.* **1994**, *6*, 1250−1257.

(17) Mathias, J. P.; Simanek, E. E.; Zerkowski, J. A.; Seto, C. T.; Whitesides, G. M. *J. Am. Chem. Soc.* **1994**, *116*, 4316−4325.

(18) Mathias, J. P.; Seto, C. T.; Simanek, E. E.; Whitesides, G. M. *J. Am. Chem. Soc.* **1994**, *116*, 1725−1736.

(19) (a) Honda, Y.; Kurihara, K.; Kunitake, T. *Chem. Lett.* **1991**, 681−684. (b) Koyano, H.; Yoshihara, K.; Ariga, K.; Kunitake, T.; Oishi, Y.; Kawano, O.; Kuramori, M.; Suehiro, K. *J. Chem. Soc., Chem. Commun.* **1996**, 1769−1770. (c) Koyano, H.; Bissel, P.; Yoshihara, K.; Ariga, K.; Kunitake, T. *Chem. Eur. J.* **1997**, *3*, 1077−1082.

(20) (a) Bohanon, T. M.; Denzinger, S.; Fink, R.; Paulus, W.; Ringsdorf, H.; Weck, M. *Angew. Chem., Int. Ed. Engl.* **1995**, *34*, 58−60. (b) Ahuja, R.; Caruso, P. L.; Möbius, W. P.; Ringsdorf, H.; Wildburg, G. *Angew. Chem., Int. Ed. Engl.* **1993**, *32*, 1033−1036. (c) Weck, M.; Fink, R.; Ringsdorf, H. *Langmuir* **1997**, *13*, 3515−3522.

(21) Huo, Q.; Russell, K. C.; Leblanc, R. M. *Langmuir* **1998**, *14*, 2174−2185.

(22) (a) Dluhy, R. A.; Mendelsohn, R. *Anal. Chem.* **1988**, *60*, 269−278. (b) Gericke, A.; Mendelsohn, R. *Langmuir* **1996**, *12*, 758−762. (c) Schmitt, L.; Bohanon, T. M.; Denzinger, S.; Ringsdorf, H.; Tampe, R. *Angew. Chem., Int. Ed. Engl.* **1996**, *35*, 317−320. (d) Adnet, F.; Liquier, J.; Taillandier, E.; Singh, M. P.; Rao, K. E.; Lown, J. W. *J. Biol. Struct.* **1992**, *10*, 565−575. (e) Mendelsohn, R.; Brauner, J. W.; Gericke, A. *Annu. Rev. Phys. Chem.* **1995**, *46*, 305−334.

(23) Flach, C. R., Gericke, A., Mendelsohn, R. *J. Phys. Chem. B* **1997**, *101*, 58−65.

(24) Blaudez, D.; Buffeteau, T.; Cornut, J. C.; Desbat, B.; Escafre, N.; Pezolet, M.; Turlet, J. M. *Appl. Spectrosc.* **1993**, *47*, 869−874.

(25) Blaudez, D.; Turlet, J. M.; Dufourcq, J.; Bard, D.; Buffeteau, T.; Desbat, B. *J. Chem. Soc., Faraday Trans.* **1996**, *92*, 525−530.

(26) Wang, Y. L.; Mebel, A. M.; Wu, C. J.; Chen, Y. T.; Lin, C. E.; Jiang, J. C. *J. Chem. Soc., Faraday Trans.* **1997**, *93*, 3445−3451.

(27) Scoponi, M.; Polo, E.; Pradella, F.; Bertolasi, V.; Carassiti, V.; Goberti, P. *J. Chem. Soc., Perkin Trans.* **1992**, *2*, 1127−1132.

(28) Sawodny, W.; Niedenzu, K.; Dawson, J. W. *J. Chem. Phys.* **1966**, *45*, 3155−3156.

(29) (a) Daimay, L. Y.; Norman, B. C.; William, G. F.; Jeanette, G. G. In *The Handbook of Infrared and Raman Charateristic Frequencies of Organic Molecules*; Academic Press: New York, 1991; p 280. (b) Reference 29a, p 300. (c) Reference 29a, p 162. (d) Reference 29a, p 142−146.

(30) Barnes, A. J.; Le Gall, L.; Lauransan, J. *J. Mol. Struct.* **1979**, *56*, 15−27.

(31) Yang, W. S.; Chen, S. G.; Chai, X. D.; Cao, Y. W.; Lu, R.; Chai, W. P.; Jiang, Y. S.; Li, T. J.; Lehn, J.-M. *Synth. Met.* **1995**, *71*, 2107−2108.